

# Real-time, Digital LAMP with Commercial Microfluidic Chips Reveals the Interplay of Efficiency, Speed, and Background Amplification as a Function of Reaction Temperature and Time

Justin C. Rolando,<sup>1</sup> Erik Jue,<sup>2</sup> Nathan G. Schoepp,<sup>1</sup> and Rustem F. Ismagilov<sup>1,2\*</sup>

<sup>1</sup>Division of Chemistry and Chemical Engineering, California Institute of Technology

<sup>2</sup>Division of Biology and Biological Engineering, California Institute of Technology  
1200 E. California Blvd., Pasadena, CA, 91125 United States of America

\*Correspondence to: [rustem.admin@caltech.edu](mailto:rustem.admin@caltech.edu)

## Table of Contents

<b>S-I</b>	<b>Summary of MATLAB script functions</b>
<b>S-II</b>	<b>Real-time data acquisition parameters</b>
<b>S-III</b>	<b>Limitations of chips used</b>
<b>S-IV</b>	<b>Calculation of peak width metrics</b> Equations S1-S2 Table S1
<b>S-V</b>	<b>Mode time to positive</b> Figure S1
<b>S-VI</b>	<b>Hardware and pre-heating considerations</b> Figure S2
<b>S-VII</b>	<b>Optimization of <i>Bst</i> 2.0 buffer composition</b> Figure S3
<b>S-VIII</b>	<b>Contributions of non-corresponding authors</b>

## S-I Summary of MATLAB script functions

In order to quantify the reactions on chips using the Poisson distribution, we needed to know the number of partitions that contained solution and the number of partitions that were empty. (It would be naïve to assume that all 20,000 partitions were loaded with solution; visual inspection shows that was rare.) We counted the total number of partitions with solution using the image of the autofluorescence of SYTO 9 dye before heating at time 0 (**Figure 2a**). SYTO 9 had uniform autofluorescence independent of template presence, making it easy to count all partitions loaded with solution.

To track the mean fluorescence intensity of each partition over time, we solved two challenges. First, when the microfluidic chip was heated (especially during the first 2 min) the chip moved. As the chip heated, it lost the initial autofluorescence from SYTO 9. Consequently, it was not possible to track this movement with the fluorescence of a single fluorophore. We solved this challenge by creating a mask (using image segmentation) that outlined each detectable partition at the chip's final position using a frame at the end of amplification. An advantage to using only the detectable partitions that met a minimum fluorescence intensity (out of a total of 20,000 partitions per chip) was reduced overall computation time because only a fraction of the total partitions were tracked in real-time.

A second challenge when tracking mean fluorescence intensity of each partition over time using only the detectable partitions is that partitions can appear to be different sizes because of differences in fluorescence intensity (dark partitions can appear artificially smaller and bright partitions can appear artificially larger). To counteract the effect of each partition having a different average intensity, we performed multi-level thresholding with tight restrictions for the area and major axis filters. We set a minimum fluorescence intensity (threshold) for each pixel at a given time and used this information to segment (define the perimeter) each individual partition. This threshold was combined with selection criteria for the area and major axis. The area filter defined the smallest and largest partitions while the major axis filter ensured that detected regions were circular. We repeated this for different threshold values and merged the resulting partitions. This technique restricted partitions to a specific size and shape while enabling detection over many intensity values.

Finally, we used the information from quantifying the number of partitions containing solution and tracking mean fluorescence of each partition over time to calculate the concentration of template in the bulk solution. To smooth the traces and reduce the noise, we first applied a Gaussian-weighted moving average filter with window length 10 frames to each intensity curve. To ensure all partitions start at zero intensity, we determined the baseline intensity by calculating the average partition intensity for selected frames after heating but prior to detectable amplification (between 2.5 min and 5 min). The baseline intensity was subtracted from all frames. Finally, we manually defined a threshold to determine whether a partition would be counted as a "positive" or "negative." Using the adjusted traces, threshold, and the total number of partitions, we determined the fraction of partitions that were "on" for any given time. Using the fraction of partitions that were "off," we calculated via the Poisson distribution the concentration of template detected in the bulk solution for any given time point. From this measurement of concentration, we can calculate the amplification efficiency by dividing the measured concentration by the known (true) concentration.

The MATLAB script described here has been deposited in the open-access online repository GitHub and may be accessed using the following direct link:  
[https://github.com/IsmagilovLab/Digital\\_NAAT\\_Analyzer](https://github.com/IsmagilovLab/Digital_NAAT_Analyzer)

## **S-II Real-time data acquisition parameters**

### **Acquiring real-time data using microscopy**

Images were acquired in 30-sec intervals on a Leica DMI-6000B (Leica, Buffalo Grove, IL, USA) with a 1.25x 0.04NA HCX PL FLUOTAR Objective (506215) and 0.55x coupler (Leica C-mount 11541544) using a 1-sec exposure through the L5 (GFP) Nomarski prism and a Hamamatsu ORCA-ER CCD camera (Hamamatsu Photonics K.K., Hamamatsu City, Shizuoka, Japan; Ref. C4742-80-12AG). Heating was performed using an integrated circuit (IC) board prototype for temperature control developed by Green Domain Design (San Diego, CA, USA). The IC board was connected to a DC power supply (Model 3670; Electro Industries, Monticello, MN, USA), a Nichrome wire (12 ohm) attached to a 5 x 25 x 25 mm aluminum block. A thermistor was mounted within the block to measure the temperature of the heating block. When the temperature of the heating block was lower than the set-point temperature, the IC board supplied current to the Nichrome wire resistive heater. With this setup, heating was achieved to  $70.0 \pm 2$  °C within 2 min. Images obtained on the microscope were processed with our MATLAB script (**Supporting Information, S-I**) using the following parameters: Area Bound [5 40] pixels, Major Axis [2 9] pixels, Threshold [250] Relative Fluorescence Units (RFU), Baseline Smoothing Frames [6 11], Masking Image Frame [175].

### **Acquiring data using a custom large-format real-time amplification instrument (RTAI)**

Images were acquired in 30-sec intervals on a custom-built, public-domain real-time amplification instrument (RTAI), described previously,<sup>30</sup> using the FAM channel with a 15-sec exposure at  $f/5.6$ . Heating was achieved using the built-in PCT-200 thermocycler, which heats to  $70.0 \pm 0.3$  °C within 70 sec. The temperature of the thermocycler block was held at 25 °C to start all reactions, with the exception of an experiment where the block was preheated to the optimal temperature (**Figure S2b**). We equipped the thermocycler with an aluminum block with two sloped planes (each set at 11°—an angle defined by the microfluidic chip manufacturer's requirements), to segregate bubbles formed during the reaction to a specifically designed bubble trap. It was advantageous to use this instrument to analyze up to six chips in parallel in a single field of view and under a uniform temperature. By running multiple chips on a real-time instrument we achieved “multiplexed” assays (wherein multiple measurements are made simultaneously). Images obtained on the RTAI were processed through our MATLAB script (**Supporting Information, S-I**) using the following parameters: Area Bound [4 12] pixels, Major Axis [2 5] pixels, Threshold [100] RFU, Baseline Smoothing frames [6 11], Masking Image Frame [175].

### **S-III Limitations of chips used**

A limitation of chips that discretize by capillary action is that solution can spread among the partitions. For example, during dLAMP quantification of extractions for three of the clinical samples, we observed spreading of one positive partition to its adjacent partitions. We attribute this spreading to liquid bridges forming among adjacent wells, resulting in transfer of the amplicon among compartments. These bridges could arise from defects in surface coatings of commercial chips or from an excess of surface active molecules present in some clinical samples. To test whether spreading was due to surface active impurities in the samples, samples were diluted in Tris-EDTA (TE) buffer and in the subsequent test, spreading was eliminated for one sample. For the remaining samples, dilution reduced the spreading enough that quantification at 10 min was not hindered, although some spreading was observed at later times. Quantification of the C:T ratio remained consistent (and the susceptibility call the same) because we use a ratiometric calculation.

### **S-IV Calculation of Peak width metrics**

The average distribution curve (averaged over three trials) was calculated for each temperature and all values normalized to the peak prominence. Time resolution was estimated to the nearest 15 second interval. Calculations were based on: [John V. Hinshaw. "How Do Your Peaks Measure Up?" Oct 01, 2013, LCGC Europe, Volume 26, Issue 10, pg 575–582.](#)

Full Width at Half Maximum was calculated at the time difference between the leading at tailing edges at 50% peak prominence.

Asymmetric factor was calculated by dividing the time between the peak prominence and the tailing edge (" $b_{0.1}$ ") by the time between the peak prominence and the leading edge at 10% peak height (" $f_{0.1}$ ").

(Eq. S1)

$$\text{Asymmetric Factor} = \frac{b_{0.1}}{f_{0.1}}$$

Tailing factor was calculated as the total peak width at 5% of the prominence (or the distance from the leading edge to the time of peak prominence (" $f_{0.05}$ ") plus the distance from the time of peak prominence to the tailing edge (" $b_{0.05}$ ")) divided by twice the distance from the leading edge to the time of peak prominence.

(Eq. S2)

$$\text{Tailing Factor} = \frac{f_{0.05} + b_{0.05}}{2f_{0.05}}$$

**Table S1. Tabular quantification of the time to threshold distribution curves.**

<i>Bst</i> 2.0						<i>Bst</i> 3.0					
Temp (°C)	Efficiency at 45 min (%)	Mode TTP (min)	FWHM (min)	Asymmetric Factor	Tailing Factor	Temp (°C)	Efficiency at 45 min (%)	Mode TTP (min)	FWHM (min)	Asymmetric Factor	Tailing Factor
64.0	64±8	9.5±0.0	2.5	10.2	14.8	64.0	57±2	8.2±0.3	3.0	8.0	14.2
66.0	78±2	9.3±0.3	2.3	7.6	11.7	66.0	61±2	7.3±0.3	2.3	5.6	11.4
68.0	78±2	9.8±0.3	2.3	7.2	14.3	68.0	71±6	7.6±0.3	2.3	6.0	9.2
70.0	66±1	11.0±0.0	2.8	8.8	9.1	70.0	69±3	6.7±0.3	1.5	7.3	3.7
						72.0	51±3	7.2±0.3	2.0	8.3	4.3
						74.0	33±9	10.2±0.6	2.8	5.7	13.1

**S-V Time to Mode Positive**

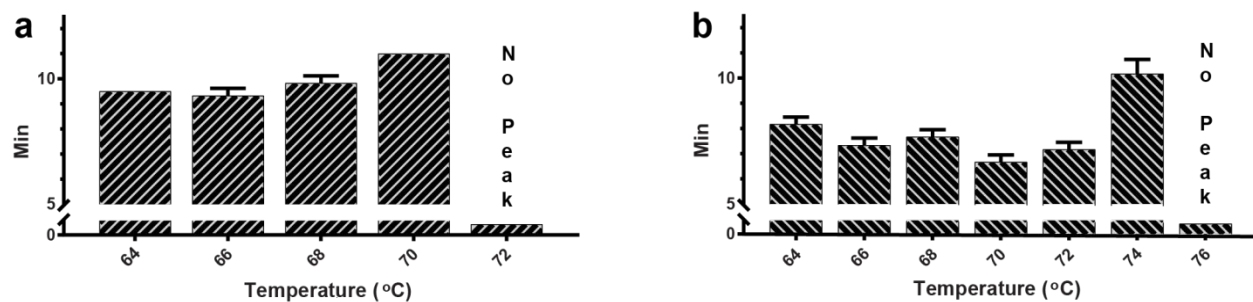


**Figure S1. Bar graphs of the time location of the peak of the distribution curve (time to mode positive) using *Bst* 2.0 (a) and *Bst* 3.0 (b). We required 15 or greater partitions turn on at a given time (0.075% of total partitions), to include the time point for the mode. Data are summarized in Table S1 in S-III.**

## S-VI Hardware and pre-heating considerations

We asked if multiple instrumentation formats could be used to collect the data and if hardware format impacted the amplification efficiency. We used the optimal conditions for *Bst* 3.0. First, we compared the performance of the large-format real-time amplification instrument (RTAI) to a wide-field microscope fitted with a heat block—a set-up that would be accessible to most laboratories. We found that the heater ramp rate was slower on the microscope than the RTAI (120 sec versus 70 sec) resulting in  $9.0 \pm 1.0$  min time to mode positive (**Figure S2a**).

Next, we looked at the effect of pre-heating using the RTAI. We compared the optimal conditions using *Bst* 3.0 and starting from 25 °C (green curve) with the same instrument and heating block already at the optimal reaction temperature of 70 °C (orange curve). When the block is preheated, we observed the mode time to threshold reduced from  $6.7 \pm 0.3$  min to  $6.0 \pm 0.0$  min (**Figure S2a**).

Next, we asked if differences in hardware configuration and the heating rates between the instruments would also correspond to differences in probability of detection. We observed significant variation in amplification efficiency (RTAI vs RTAI with preheating  $P = 0.002$ ; RTAI vs microscope with heater  $P = 0.031$ , RTAI with preheating vs microscope with heater  $P < 0.001$ ) and concluded that heating rate may impact probability of amplification (**Figure S2b**). Hence, all comparisons made in this study were instrument specific. Though it remains to be tested, we suspect more precise hardware, with improved heating control, could improve device performance.

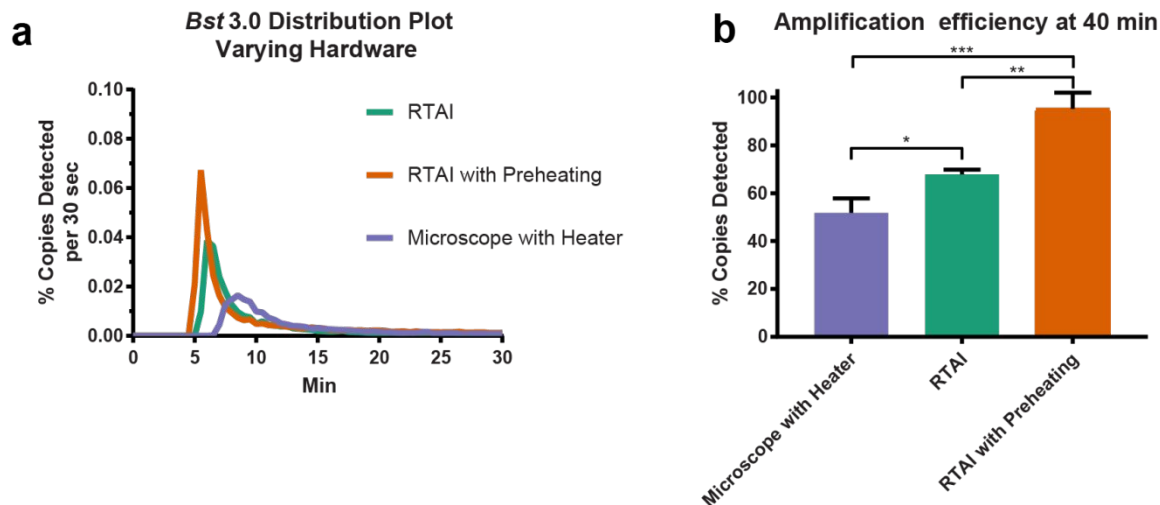


**Figure S2. Effect of hardware and heating on (a) the distribution in time to fluorescence threshold and (b) quantification of amplification efficiency (mean percentage copies detected  $\pm$  S.D.) at 40 min.**

### S-VII Optimization of *Bst* 2.0 buffer composition

Following the protocol described previously<sup>18</sup>, buffer conditions for *Bst* 2.0 were optimized in bulk at 713 copies/uL (e.g. ~4,280 or 0 copies per 6  $\mu$ L reaction). Optimal buffer composition was selected based on fastest bulk time to positive.

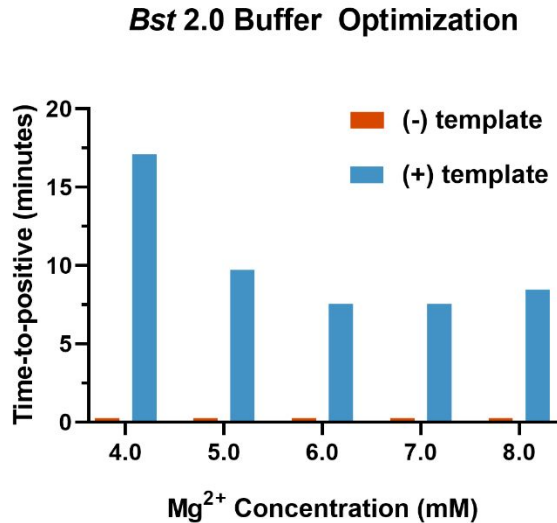


**Figure S3. Magnesium optimization for *Bst* 2.0. A value of 0.25 indicates that no amplification was observed. Amplification was performed at 67.5° C. N=1 for all TTP values.**

### S-VIII Contributions of non-corresponding authors

J.C.R. conceptualized the method, generated and analyzed data. Wrote the paper, constructed figures, and performed all revisions.

E.J. wrote the MATLAB software script for automated analysis of digital LAMP image sequences. Provided minor input to experimental design; and minor edits and inputs to the figures and manuscript.

N.G.S. prepared and quantified nucleic acid stocks. Optimized buffer conditions for *Bst* 2.0. Provided minor input to experimental design and minor edits and inputs to the figures and manuscript.